# Polar order in columnar phase made of polycatenar bent-core molecules

Ewa Gorecka,[a,*] Damian Pociecha,[a] Joanna Matraszek,[a] Jozef Mieczkowski,[a] Yoshio Shimbo,[b] Yoichi Takanishi,[b] Hideo Takezoe [b]

[a] Chemistry Department, Warsaw University, Al. Zwirki i Wigury 101, 02-089 Warsaw, Poland, * e-mail: gorecka@chem.uw.edu.pl
[b] Department of Organic and Polymeric Materials, Tokyo Institute of Technology, O-okayama, Meguro-ku, Tokyo 152-8552, Japan

PACS: 61.30.Cz, 64.70.Md, 77.84.Nh, 77.22.Gm

The columnar phases made of polycatenar molecules with bent shaped mesogenic core are studied. The polar order in this system is associated with the change of the column building blocks from flat discs ($Col_h$ phase) into cones ($Col_hP_A$ phase), which allows for axial polarization of the columns. The nature of $Col_h$ and $Col_hP_A$ phase transition changes from the first order for short homologues to continuous for the longest one. This can be attributed to decreasing intercolumnar interactions due to broadening of the columnar scaffold made of partially melted terminal alkyl chains. Decrease of intercolumnar interactions is also responsible for strong increase of pretranstional fluctuations in the $Col_h$ phase. The mesophase observed for longest homologues is reminiscent of relaxor phase observed for solid crystals.

## Introduction

The polar order in soft matter has been extensively studied for liquid crystals. For a long time polar order was associated with breaking of the chiral symmetry, this approach has been widely applied to obtain ferroelectric [1] and antiferroelectric [2] lamellar and even columnar mesophases [3, 4]. In 1996, for the first time, a switchable polar smectic phase was reported also in an achiral molecular system [5, 6], where order of dipoles resulted from restricted molecular rotation due to the steric interactions of bent-core molecules. Recently ferroelectric switching has been also reported in columnar phases made of achiral molecules, for these materials the spontaneous electric polarization along the columns originates in soft intermolecular interactions: the net of hydrogen bonds [7, 8] or assembling of bent-core polycatenars (molecules having multiple terminal chains) into cone-like units [9]. Here we report complex thermodynamics of polar order development in homologous series of polycatenar compounds. In studied materials the polar structure grows from a paraelectric phase either through discontinuous or continuous phase transition. In case of the discontinuous phase transition the antiferroelectric phase is obtained below the paraelectric one, while the properties of the polar phase that enters through continuous phase transition in many aspects remind that of disordered relaxor phases [10].

## Results and Discussion

In all materials of the studied homologous series (Fig. 1, table 1) below the isotropic phase three columnar phases were detected: $Col_h$ phase, $Col_hP_A$ phase and $Col_X$. The $Col_h$ phase is paraelectric while the $Col_hP_A$ phase is axially polar and switchable under electric field. The rather high threshold field is required for switching; in n=16 homologue saturated current peak is obtained for about 20 V μm$^{-1}$ and even higher fields are necessary for shorter homologues. For n=16 material the spontaneous polarization is ~250 nC cm$^{-2}$ and decreases to zero on approaching the $Col_h$ phase. Previous X-ray studies confirmed strictly hexagonal arrangement of columns for both $Col_h$ and $Col_hP_A$ phases [9]. Assuming 1 g cm$^{-3}$ density of material it could be deduced that in all phases the column stratum is made of 3-4 molecules, which are arranged into flat discs in $Col_h$ phase and into cones in the $Col_hP_A$ phase (Fig. 1). The change of column building blocks, from flat discs into cones is followed by monitoring the temperature variation of Bragg reflection with index (10), related to the inter-column distance. This distance decreases profoundly at $Col_h$ - $Col_hP_A$ phase transition (Fig. 2), as expected for discs deforming into cones. The decrease is either stepwise (for homologues n=8, 12, 14) or continuous (homologue n=16). The cone angle obtained by comparing the column diameters in the $Col_h$ and $Col_hP_A$ phases near the transition point is in a range of 130-140 deg. for all homologues. The crossover from discontinuous to continuous $Col_h$ - $Col_hP_A$ phase transition with elongation of terminal chains is also clearly visible in calorimetric studies (Fig. 3). For shortest homologue, n=8, at the $Col_h$ - $Col_hP_A$ phase transition a sharp peak due to the latent heat with almost no heat capacity ($c_p$) anomalies is observed, as well as pronounced hysteresis of the transition temperature ($T_c$) for cooling and heating scans. The hysteresis diminishes, and the peak develops the $c_p$ wings for longer homologues and for n=16 material no hysteresis and broad $c_p$ anomaly at both side of $T_c$ are detected. Strong $c_p$ anomalies are characteristic of continuous (second order) phase transition, the temperature hysteresis for heating and cooling scans is possible only for discontinuous (first order) phase transition. The polar instability associated with $Col_h$ - $Col_hP_A$ phase transition is clearly seen in dielectric studies. For all homologues the monodispersive relaxation process is observed in the $Col_h$ phase (Fig. 4), that strength considerably increases near the phase transition to the $Col_hP_A$ phase. Most probably the relaxation mode originates in fluctuations deforming the non-polar flat discs into polar cones, hereafter called *umbrella* mode. This assumption is justified as instantaneous phase structure that would be imposed by such fluctuations is polar and corresponds to lower temperature phase structure. The temperature variation of the relaxation frequency of the *umbrella* mode depends on the nature of the $Col_h$ - $Col_hP_A$ phase transition. For homologues n=8 and n=12, which exhibit strongly first order phase transition, the *umbrella* mode relaxation frequency, $f_r$, follows Vogel–Fulcher (VF) dependence [11], $f_r \equiv f_{VF} = f_0 e^{-\frac{D}{T-T_g}}$, where $f_0$ and $D$ are constants and $T_g$ is the glass transition temperature. The VF model is generalization of Arrhenius model, and is used for systems in which complete freezing of molecular motions occurs at $T_g > 0$ K. For both n=8 and n=12 homologues $T_g$ obtained by fitting the VF equation to experimental data is several degrees below $T_c$. For homologue n=14 the relaxation frequency of the *umbrella* mode shows small departure from VF behavior in low temperature range of the $Col_h$ phase, its decrease is faster than predicted by VF behavior. For homologue n=16, on lowering the temperature, approaching of the polar phase is manifested by rapid dumping of relaxation frequency and strong deviation from VF dependence. Near the phase transition $f_r$ can be best described by superposition of VF and Curie-Weiss (CW) dependence, $f_r = A(T - T_s)\, f_{VF}$ (see inset of Fig. 4), that characterizes systems in which the energy barrier for dipole re-orientation under an electric field depends on temperature [11]. Such a coexistence of the critical slowing down and glassy freezing has been often considered for solid relaxors [12]. For materials n=8-14 in $Col_hP_A$ phase no any low-frequency relaxation process could be detected, the *umbrella* mode is quenched exactly at the temperature at which the heat flow peak is observed in DSC scan and the diameter of columns discontinuously changes. Contrary to shorter homologues, in material n=16 the relaxation process is not suppressed at the $Col_h$ - $Col_hP_A$ phase transition, it can be seen over several degrees below $T_c$. The temperature dependence of the dielectric response measured at different frequencies (Fig. 5) exhibits characteristic shifts of dielectric susceptibility maximum position and value, which further confirms existence of some slow, polarly active fluctuations in lower temperature phase.

The discs deformation into cones can be detected also by optical methods (Fig. 6). All observed phases are optically uniaxial with optical axis along the column axis. In the $Col_hP_A$ phase the optical birefringence decreases relative to $Col_h$ phase, as discs deformation increases the refractive index component along the column and decreases the component transverse to the column axis, simple calculations show that the birefringence changes with cone angle $\beta$ as $3\cos^2(\frac{\pi-\beta}{2})-1$. In all materials the $Col_hP_A$ phase is nearly optically isotropic that suggest the cone angle close to 110 deg. Along with results of X-ray studies, the change of birefringence at $Col_h$ - $Col_hP_A$ phase transition is stepwise for compounds n = 8-14, and the step decreases on elongation of the terminal groups. For n=16 homologue continuous change of birefringence through the phase transition is observed. The birefringence measurements are also used to monitor the *umbrella* fluctuations deforming the discs in $Col_h$ phase. The straightforward calculations (analogues to that performed for SmA phase [13, 14]) show that the birefringence is influenced by *umbrella* fluctuations as $\Delta n(T) = \Delta n_0(T)\left(1 - 3/2 < (\delta\theta)^2 >\right)$, where $\pi - 2\,\delta\theta$ is the instantaneous cone angle $\beta$ (Fig. 1) and $\Delta n_0(T)$ is non-critical part of birefringence. In the $Col_h$ phase, with decreasing temperature, the background part $\Delta n_0(T)$ increases as the orientational order in the column increases. Along with growing the *umbrella* fluctuations near the phase transition, the birefringence deviates downward from the extrapolation of data obtained far above the transition temperature (inset in Fig. 6). It can be clearly seen (Fig. 6) that $<(\delta\theta)^2>$ increases with increasing homologue number, the deviation is pronounced for homologue n=16, whereas only small deviation emerges for n=8 compound before making the phase transition to $Col_hP_A$. Although the exact analysis of fluctuations is difficult, as their magnitude depend on the chosen background $\Delta n_0(T)$, for n=16 material the average amplitude of pretransitional fluctuations in the $Col_h$ phase, $\sqrt{< (\delta\theta)^2 >}$, as high as 30 degrees can be estimated. There are also visible pretransition changes of birefringence in the $Col_hP_A$ phase near $T_c$. In this phase, however, it is not possible to separate the part of birefringence changes due to the mean field change of cone angle and due to cone angle fluctuations.

Finally, the SHG method has been used to monitor the polar properties of the phases. It should be emphasized that all phases are SHG silent in the ground state. The result is consistent with paraelectric properties of the $Col_h$ phase and the structure with compensated polarization of the $Col_hP_A$ phase. The SHG signal becomes visible in the $Col_h$ phase upon applying an electric field, which deforms the discs and induces finite polarization. The SHG intensity follows square of applied field, as predicted for paraelectric materials [15]. With decreasing temperature in the $Col_h$ phase the induced nonlinear polarization becomes larger and attains maximal SHG intensity near the $Col_h$ -

$Col_hP_A$ phase transition temperature (Fig. 7) as at this temperature susceptibility of the discs to the deformation is the highest. On further cooling in the $Col_hP_A$ phase the signal diminishes due to insufficient voltage to assure full switching into ferroelectric state. The difference between n=8 and n=16 compounds is clearly seen in Fig. 7; the maximum of SHG signal appears at the phase transition for n=8 and disappears abruptly below the transition temperature, whereas for n=16 it appears below phase transition temperature and diminishes gradually on cooling. The broad temperature range in $Col_hP_A$ phase of n=16 homologue, which is SHG active under applied electric field may originate from the existence of polar clusters.

**Conclusions**

Summarizing, the experimental results show that $Col_h$ - $Col_hP_A$ phase transition is associated to the change of the column building blocks from flat discs into cones, which allows for axial polarization of the columns in the $Col_hP_A$ phase. In the $Col_hP_A$ phase columns are arranged into hexagonal lattice, with spontaneous electric polarization along the columns. The lack of SHG signal and low dielectric response together with polarization switching in electric field unambiguously point to antiferroelectric structure of the phase. However, the simple antiferroelectric arrangement of columns should be excluded as it is incompatible with hexagonal lattice of columns [16]. The model of $Col_hP_A$ phase, described previously [9], involves breaking of the columns and forming blocks with reversed polarization direction. To fulfill close packing requirements, the blocks are shifted by half the lattice period in the plane normal to the columns axis. The other model that could be also considered assumes harmonic modulations of cone angle

$\beta$, thus polarization and density, along the column axis. In this model the antiferroelectric hexagonal lattice frustration is avoided by shifting the phase of the modulation between columns. The exact 3-D structure of the $Col_hP_A$ phase is still to be elucidated.

The presented results of X-ray, dielectric and optical studies confirmed that development of the polar order depends on column interactions. Apparently, with broadening of columns alkyl shells formed by partially melted terminal chains, the steric interactions between columns weaken and the columns become more susceptible to deformation. In result the softening of polar lattice motions in $Col_h$ phase is observed together with growing correlation length for dipole-dipole interactions within the column; finally rising fluctuations drive the $Col_h$ - $Col_hP_A$ phase transition into the second order for n=16 homologue. For n=16 material evolution from paraelectric to polar phase is characterized by diffused, rather than abrupt, structural phase transition. The presence of strong, polar low-frequency mode and the lack of permanent polarization in zero field state (proven by absence of SHG signal) in $Col_hP_A$ phase may suggest that, contrary to shorter homologues, the phase has irregular antiferroelectric structure made of ferroelectric clusters with random distribution of polarization. In disordered ferroelectric regions of the $Col_hP_A$ phase the dielectric relaxation occurs due to the polarization reversal, also domain boundary motions contribute to dielectric response. It should be stressed that although the physical properties of $Col_hP_A$ phase of n=16 material seems to be reminiscent of solid relaxors, their origins are much different. Most solid relaxor phases are believed to be caused by compositional fluctuations [17] or defects [18].

**Experimental**

The detailed synthetic procedure for studied materials will be described elsewhere. X-ray experiments were performed with modified DRON diffractometer ($CuK_{\alpha}$ line) in reflection mode from one surface free sample. The temperature stability was controlled with accuracy 0.1 K. Calorimetric studies were conducted with Perkin Elmer DSC-7 apparatus, with scanning rates ±5 K $min^{-1}$. Dielectric measurements were done with Solartron Impedance Analyzer SI1260, samples were sandwiched in ITO coated glass cells, 2-10 μm thick, and put in Mettler FP82HT hot stage for temperature control. The same samples were used for light transmission and birefringence measurements, which were performed with setup based on He-Ne laser, photoelastic modulator PEM90, lock-in-amplifier EG&G 7265 and photodiode FLCE PIN20. SHG intensity was observed by the oblique incidence (45 deg.) of a *p*-polarized fundamental wave from a Nd:YAG laser (Surelite I; SLI-10 1064 nm, 10 Hz, 2 mJ/pulse) to the 5 μm cells. *p*-polarized SHG was detected from the transmission direction at the maximum voltage of the triangular wave (10 Hz, 30 Vpp $\mu m^{-1}$) applied along the substrate normal.

**Acknowledgements**

The work was supported by KBN Grant No 4T09A 00425.

**References**

[1] R. Meyer, L. Liebert, L. Strzelecki, P. J. Keller, *Phys. France, Lett.* **36**, L69, (1975).

[2] A. D. L. Chandani, E. Gorecka, Y. Ouchi, H. Takezoe, A. Fukuda, *Jpn. J. Appl. Phys.* **28**, L1265, (1989).

[3] H. Bock, W. Helfrich, *Liq. Cryst.* **12,** 697, (1992).

[4] G. Scherowsky, X. H. Chen, *Liq. Cyst.* **24**, 157, (1998).

[5] T. Niori, T. Sekine, J. Watanabe, T. Furukawa, H. Takezoe, *J. Mater. Chem.* **6**, 1231, (1996).

[6] C. Tschierske, G. Dantlgraber, *Pramana* , **61**, 455, (2003).

[7] K. Kishikawa, S. Nakahara, Y. Nishikawa, S. Kohmoto, M. A. Yamamoto, *J. Am. Chem. Soc.* **127**; 2565, (2005).

[8] Y. Okada, S. Matsumoto, Y. Takanishi, K. Ishikawa, S. Nakahara, K. Kishikawa, H. Takezoe, *Phys. Rev. E* **72**, 020701, (2005).

[9] E. Gorecka, D. Pociecha, J. Mieczkowski, J. Matraszek, D. Guillon, B. Donnio, *J. Am. Chem. Soc.* **126**, 15946, (2004).

[10] L. E. Cross, *Ferroelectrics* **76**, 241, (1987).

[11] M. E. Line and M. Glass, *Principle and Applications of Ferroelectric and Related Materials* (Oxford University Press, Oxford, 2001).

[12] B. E. Vugmeister, H. Rabitz, *Phys Rev B* **61**, 14448, (2000).

[13] K. C. Lim, J. T. Ho, *Phys. Rev. Lett.* **40**, 1576, (1978).

[14] M. Skarabot, K. Kocevar, R. Blinc, G. Heppke, I. Musevic, *Phys. Rev. E*, **59**, 1323, (1999).

[15] R. W. Terhune, P. D. Maker, C. M. Savage, *Phys. Rev. Lett.* **8,** 404, (1962).

[16] M. Harris, *Nature* **399**, 311, (1999).

[17] H.Z. Jin, J. Zhu, S. Miao, X.W. Zhang, Z.Y. Cheng *J. App. Phys.* **89,** 5048, (2001).

[18] Y. Yoneda, N; Matsumoto, H. Terauchi, N. Yasuda, *J. Phys.: Condens. Matter.* **15**, 467, (2003).

**Table 1. Phase transition temperatures (°C) and, in parentheses, their thermal effects (J g$^{-1}$) for studied materials.**

| n | m.p. | $Col_X$ | | $Col_hP_A$ | | $Col_h$ | | Iso |
|---|---|---|---|---|---|---|---|---|
| 8 | 89.6 (11.6) | • | 128.1 (0.1) | • | 147.3 (1.8) | • | 189.5 (1.0) | • |
| 12 | 65.0 (15.5) | • | 83.8 (6.6) | • | 137.2 (1.5) | • | 197.4 (1.2) | • |
| 14 | 34.0 (17.1) | • | 83.7 (6.5) | • | 122.5 (1.1) | • | 187.3 (0.9) | • |
| 16 | 58.2 (20.3) | • | 90.2 (8.2) | • | 123.2 (1.5) | • | 174.0 (0.9) | • |

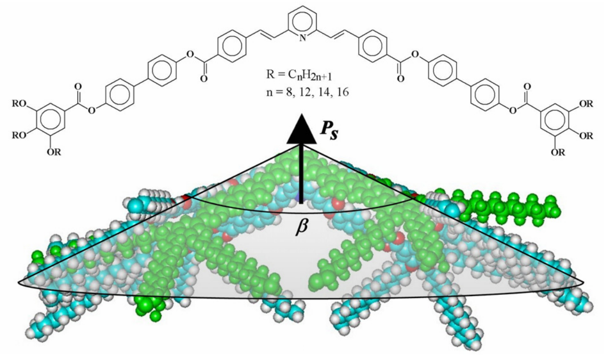


**Figure 1. General formula of studied polycatenar compounds. Below arrangement of molecules into cone-like unit is shown, $\beta$ denotes the cone angle. Cone units are arranged in columns with non-compensated electric polarization $P_s$.**

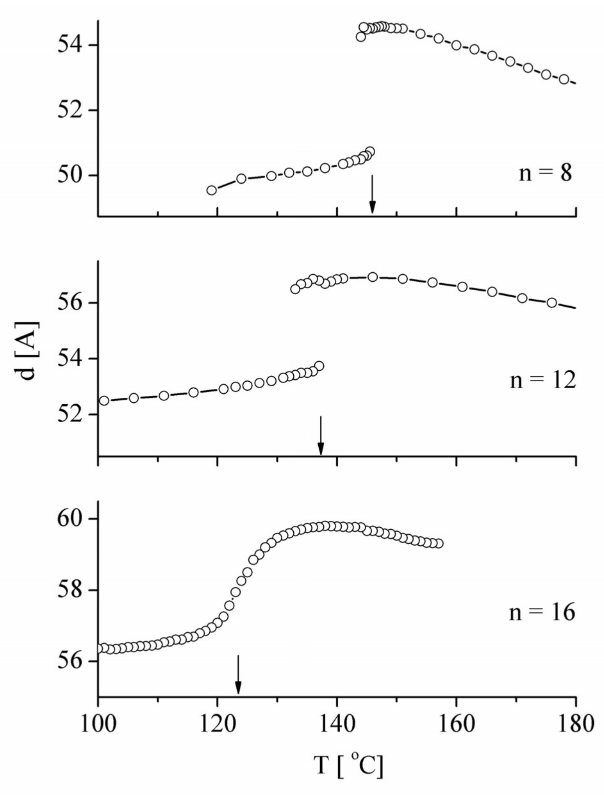


**Figure 2. Temperature dependence of (10) Bragg signal (measured on cooling) reflecting changes of the columns diameter, discontinuous change is observed at the $Col_h$ - $Col_hP_A$ phase transition for n=8, 12, while for homologue n=16 the variation is continuous. Arrows indicate the $Col_h$ - $Col_hP_A$ phase transition temperature obtained from DSC measurements.**

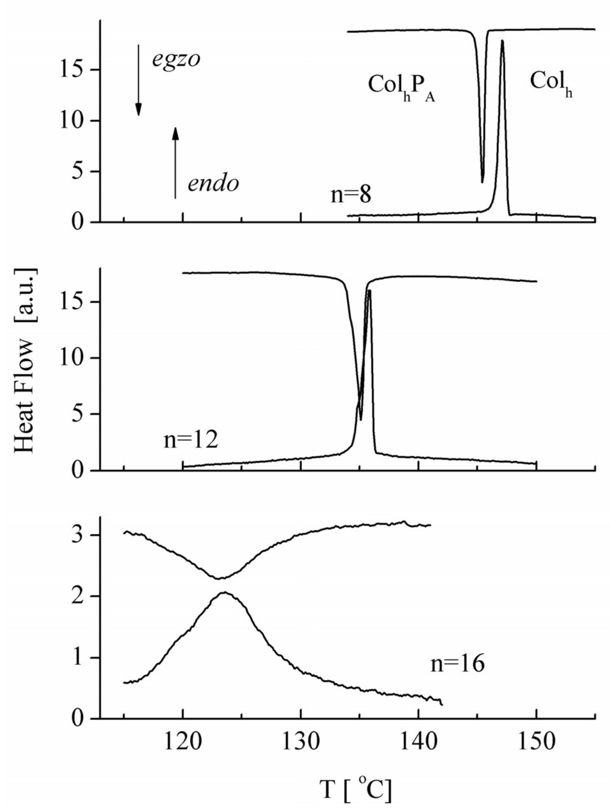


**Figure 3. DSC heat flow signals for homologues *n* = 8, 12 and 16. The signals develop $c_p$ wings and the hysteresis for heating and cooling scans diminishes as the terminal chains get longer.**

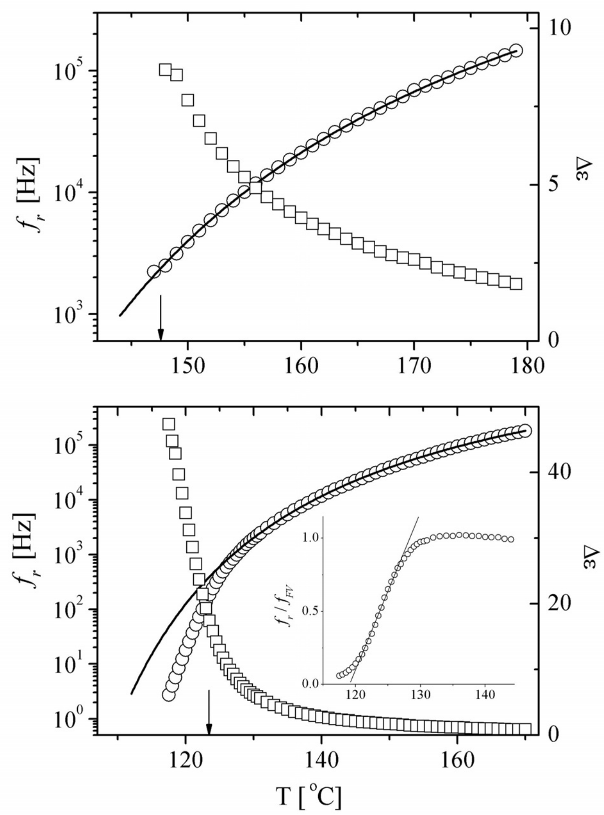


**Figure 4. Relaxation frequency (circles) and dielectric strength (squares) of '*umbrella*' mode in the $Col_h$ phase vs. temperature for homologues *n*=8 (upper graph) and *n*=16 (lower graph). The lines represent fits to the VF dependence. Arrows indicate the $Col_h$ - $Col_hP_A$ phase transition temperature obtained from DSC measurements. For n=16 in the vicinity of $T_c$ cross-over to the Curie-Weiss dependence takes place, as shown in the inset.**

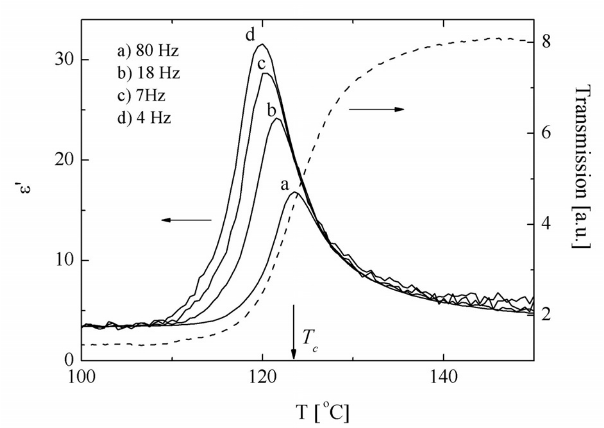


**Figure 5. Dielectric constant measured at different frequencies and simultaneously measured light transmission through a confocal domain in 3 micron thick cell for homologue n=16. The high dielectric response is still visible below the $T_c$ temperature.**

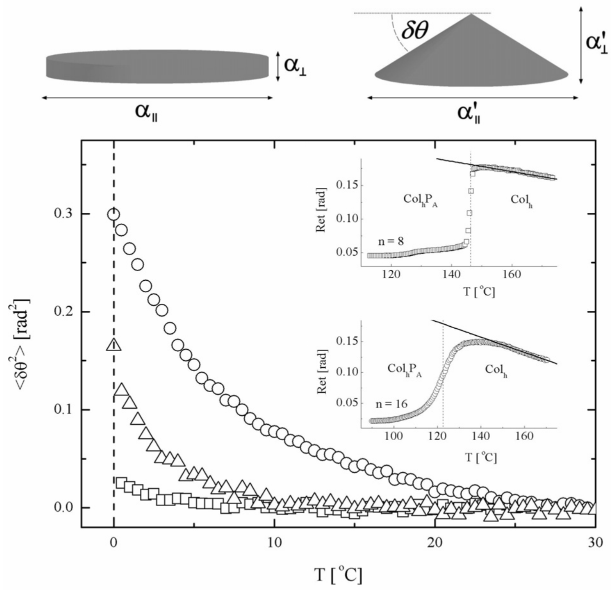


**Figure 6. Schematic drawing of column building blocks: discs and cones. The change from flat disk into cone results in change of polarisability :**
$\alpha'_{\parallel}-\alpha'_{\perp}=(\alpha_{\parallel}-\alpha_{\perp})(3/2\cos^2\delta\theta-1/2)$ **and thus reduces the birefringence.**
***below:*** **Mean square fluctuations of tilt angle vs. temperature in the $Col_h$ phase on approaching transition to the $Col_hP_A$ phase, deduced from the birefringence measurements for homologues *n*= 8 (squares), *n*=12 (triangles) and *n*=16 (circles). In the inset optical retardation vs. temperature measured in 3.2 μm cell for the light propagating along the direction inclined by 30 degree from the column axis. Solid lines show non-critical part of retardation.**

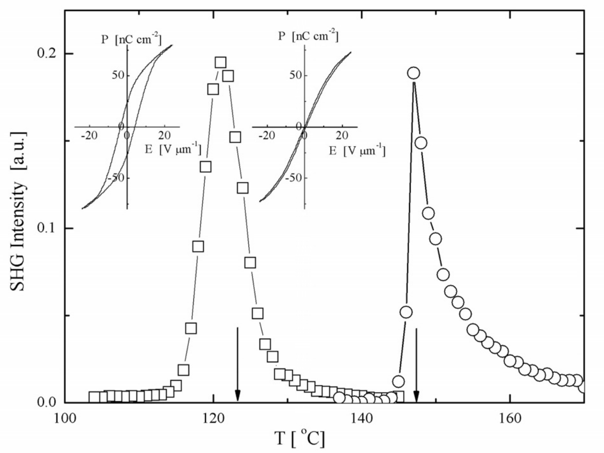


**Figure 7.** **Intensity of SHG signal vs. temperature for homologue *n*=8 (circles) and *n*=16 (squares). The SHG signal increases in $Col_h$ phase due to softening of the *umbrella* mode. Note the different signal diminishing rates in *n*=8 and *n*=16 compounds. In the insets polarization hysteresis loop measured at 20 Hz in the $Col_hP_A$ (at $T$-$T_c$ = -2 K) and $Col_h$ (at $T$-$T_c$ = 4 K) phases of *n*=16 compound showing different origins of electric field induced SHG signal in $Col_hP_A$ phase (spontaneous electric polarization) and in $Col_h$ phase (induced electric polarization). Single hysteresis loop in $Col_hP_A$ phase is observed because of too slow relaxation to antiferroelectric ground state.**